UCSF
UC San Francisco Previously Published Works

Title

Biomechanical and Hemodynamic Measures of Right Ventricular Diastolic Function: Translating Tissue Biomechanics to Clinical Relevance

Permalink

https://escholarship.org/uc/item/6wk2r053

Journal

Journal of the American Heart Association, 6(9)

ISSN

2047-9980

Authors

Jang, Sae
Vanderpool, Rebecca R
Avazmohammadi, Reza
et al.

Publication Date

2017-09-22

DOI

10.1161/jaha.117.006084

Peer reviewed

eScholarship.org Powered by the California Digital Library
University of California

ORIGINAL RESEARCH

Biomechanical and Hemodynamic Measures of Right Ventricular Diastolic Function: Translating Tissue Biomechanics to Clinical Relevance

Sae Jang, MD; Rebecca R. Vanderpool, PhD; Reza Avazmohammadi, PhD; Eugene Lapshin, BS; Timothy N. Bachman, MS; Michael Sacks, PhD; Marc A. Simon, MD

***Background*—**Right ventricular (RV) diastolic function has been associated with outcomes for patients with pulmonary hypertension; however, the relationship between biomechanics and hemodynamics in the right ventricle has not been studied.

***Methods and Results*—**Rat models of RV pressure overload were obtained via pulmonary artery banding (PAB; control, n=7; PAB, n=5). At 3 weeks after banding, RV hemodynamics were measured using a conductance catheter. Biaxial mechanical properties of the RV free wall myocardium were obtained to extrapolate longitudinal and circumferential elastic modulus in low and high strain regions (E_1 and E_2, respectively). Hemodynamic analysis revealed significantly increased end-diastolic elastance (E_{ed}) in PAB (control: 55.1 mm Hg/mL [interquartile range: 44.7–85.4 mm Hg/mL]; PAB: 146.6 mm Hg/mL [interquartile range: 105.8–155.0 mm Hg/mL]; *P*=0.010). Longitudinal E_1 was increased in PAB (control: 7.2 kPa [interquartile range: 6.7–18.1 kPa]; PAB: 34.2 kPa [interquartile range: 18.1–44.6 kPa]; *P*=0.018), whereas there were no significant changes in longitudinal E_2 or circumferential E_1 and E_2. Last, wall stress was calculated from hemodynamic data by modeling the right ventricle as a sphere: $\left(\text{stress} = \frac{\text{Pressure}\times\text{radius}}{2\times\text{thickness}}\right)$.

***Conclusions*—**RV pressure overload in PAB rats resulted in an increase in diastolic myocardial stiffness reflected both hemodynamically, by an increase in E_{ed}, and biomechanically, by an increase in longitudinal E_1. Modest increases in tissue biomechanical stiffness are associated with large increases in E_{ed}. Hemodynamic measurements of RV diastolic function can be used to predict biomechanical changes in the myocardium. **(*J Am Heart Assoc*. 2017;6:e006084. DOI: 10.1161/JAHA.117.006084.)**

Key Words: diastolic dysfunction • pressure–volume relationship • pulmonary hypertension • right ventricle • stiffness

Right ventricular (RV) failure is a major cause of mortality in patients with pulmonary hypertension (PH).[1–5] Although measures of systolic RV function have been correlated with poor clinical outcomes, a growing body of literature is beginning to show that diastolic RV function is also implicated and may even be a stronger predictor of outcomes. RV failure, for example, has been shown to have independent, incremental prognostic value in PH caused by left heart failure, the most prominent type of PH.[6] Other markers such as hemodynamic RV diastolic stiffness (β) and end-diastolic elastance (E_{ed}) have been shown to predict clinical prognosis in PH.[7–9]

Although RV failure has been linked to clinical prognosis, the mechanisms of RV failure in PH are unclear. Prior studies have examined the histological alterations of RV and pulmonary artery tissue in pulmonary arterial hypertension (PAH) patients, revealing increased cardiomyocyte cross-sectional area and collagen deposition.[9,10] On a cellular level, cardiomyocyte remodeling, as seen in explanted hearts of patients with severe PAH requiring heart or lung transplantation, has been studied biomechanically. An increase in intrinsic RV sarcomeric stiffness was found along with increased total and passive tension of myocytes, and no significant contribution of actin–myosin interaction to passive

From the School of Medicine (S.J., M.A.S.), School of Arts & Sciences (E.L.), Heart and Vascular Institute (M.A.S.), Vascular Medicine Institute (T.N.B., M.A.S.), and Department of Bioengineering (T.N.B., M.A.S.), University of Pittsburgh, PA; Department of Medicine, University of Arizona, Tucson, AZ (R.R.V.); Institute for Computational Engineering and Sciences, University of Texas at Austin, TX (R.A., M.S.).

Correspondence to: Marc A. Simon, MD, Heart & Vascular Institute, University of Pittsburgh, Scaife Hall S-555, 200 Lothrop Street, Pittsburgh, PA 15213. E-mail: simonma@upmc.edu

Received March 23, 2017; accepted July 20, 2017.

© 2017 The Authors. Published on behalf of the American Heart Association, Inc., by Wiley. This is an open access article under the terms of the Creative Commons Attribution-NonCommercial-NoDerivs License, which permits use and distribution in any medium, provided the original work is properly cited, the use is non-commercial and no modifications or adaptations are made.

Clinical Perspective

What Is New?

- Right ventricular pressure overload in rats resulted in an increase in diastolic myocardial stiffness reflected both hemodynamically, by an increase in end-diastolic elastance, and biomechanically, by an increase in longitudinal elastic modulus.
- We relate, for the first time, right ventricular myocardial tissue biomechanics to clinically relevant hemodynamics.
- We present a new stress–pressure loop to relate hemodynamic data to calculated biomechanical properties throughout the cardiac cycle.

What Are the Clinical Implications?

- Clinically measurable hemodynamics of the right ventricle can be used to predict biomechanical changes in the myocardium.
- The link between hemodynamics and biomechanics allows for clinical translation of physiologically relevant tissue biomechanical markers of cardiac modeling to assess disease severity and to guide development of novel therapies.
- The stress–pressure loop provides a new method to dynamically monitor biomechanical changes of the myocardium in various physiological states and through disease progression and treatment.
- Myofiber remodeling and myocardial stiffening in right ventricular diastolic dysfunction is a therapeutic target of interest.

tension.[9] These analyses elicited important information about the mechanism of stiffness at the myocardial cellular level and suggest new targets of therapy.

Translating cellular biomechanics insight to the tissue level has been more challenging and requires animal models. We previously studied the biomechanical stiffness of the RV myocardium at the tissue level and related this to tissue remodeling.[11] In this pulmonary artery banding (PAB) model of chronic pressure overload in the rat, we found RV dilatation and deterioration of diastolic function, as measured by increased end-diastolic pressure, along with increases in thickness and mass of the RV free wall myocardium, all of which were associated with myocyte hypertrophy but not with increased fibrosis, similar to what others have reported.[12,13] Myofiber orientation was significantly altered to align in 1 direction, and these changes were associated with increased tissue stiffness preferentially in the same direction. Tissue stiffening was found to occur only in the portion of the stress–strain curve dominated by myofibers, as opposed to collagen. In these biomechanical analyses of tissue stiffness, *stress* is defined as the amount of force applied over an area of an object, and *strain* is the relative change in size of an object caused by external forces. The ratio of these 2 parameters together (stress divided by strain, or elastic modulus [represented as E]) represents stiffness, that is, the amount of force required to deform the tissue. Our prior study showed a significant difference in the stress–strain curvilinear relationship in which the low stress/low strain portion of the curve (E_1) shifted upward (more stress required for any given strain), which is known to correspond to myocardial stretch, whereas there was no change in the slope of the high stress/high strain region (E_2), which corresponds to collagen stretch.[11,14,15]

As the next step in translating the RV tissue biomechanical findings to clinical relevance, we sought to relate myocardial tissue biomechanics to a hemodynamically derived measure of diastolic function. More specifically, we examined parameters representing myocardial stiffness to determine whether a biomechanical change in tissue stiffness is reflected by a hemodynamic measure of stiffness.

Methods

Progressive PH imposes a pressure overload on the right ventricle and can be represented by the PAB model. The experimental protocol was approved by the University of Pittsburgh institutional animal care and use committee (protocol 13021226) and conformed to the Guide for the Care and Use of Laboratory Animals (US National Institutes of Health).

PAB Procedure

RV pressure overload was induced in 5 Sprague-Dawley rats by increasing the pulmonary artery resistance via a surgical clip, as we described previously.[11,16] Briefly, animals were anesthetized with 5% isoflurane and intubated to a mechanical ventilator. The midthoracic aorta was exposed via a lateral incision. A surgical clip was placed around the pulmonary artery, and the tightness was adjusted to reach RV maximum systolic pressure >50 mm Hg. The catheter was removed. The chest was closed and sutured. The animal was extubated and observed continuously for 2 hours after the procedure and daily afterward for the first week.

In Vivo Hemodynamic Measurement

Hemodynamic analysis was performed in normal controls (n=7) and in PAB animals 3 weeks after banding. Animals were intubated, and the thorax was exposed again to access the right ventricle. A conductance pressure–volume catheter was inserted through the RV free wall into the right ventricle and positioned in the center of the ventricle where there were no

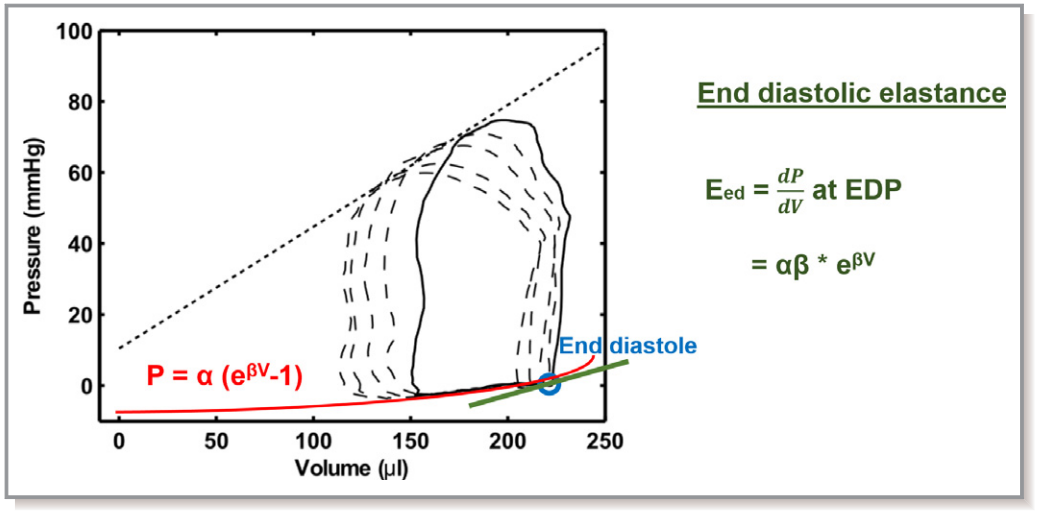

Figure 1. Diastolic function was determined by fitting the diastolic phase of a pressure–volume loop with an exponential function. E_{ed} (end-diastolic elastance) is the slope of this exponential curve at the end of diastole or at EDV. β indicates diastolic stiffness; dP/dV, change in pressure per change in volume; EDP, end-diastolic pressure; EDV, end-diastolic volume; P, pressure; V, volume.

artifacts in RV pressure–volume waveform. Pressure and volume were recorded at steady state and when the vena cava was occluded.[11,16–19] Rats were euthanized via inhalation of isoflurane. The hearts were removed and placed in cardioplegic solution.[20] The RV free wall was dissected from each heart and analyzed, as described in Biaxial Biomechanical Evaluation.

Diastolic Function Pressure–Volume Analysis

Beginning diastole was defined by minimum pressure, and end diastole was defined by the maximum of the second derivative of pressure. To avoid measurement error caused by variance in positioning the RV catheter, minimum beginning diastolic pressure (shown as BDP) was normalized to 1 mm Hg, and maximum end-diastolic volume (shown as EDV) was normalized to 1.5 mL for each rat such that $P_{normalized}=P_{measured}-(BDP_{min}-1\ mm\ Hg)$ and $V_{normalized}=V_{measured}+(1.5\ mL-EDV_{max})$.[9] Diastolic stiffness β was calculated by fitting a nonlinear exponential curve $P=\alpha\ (e^{\beta V}-1)$ through the diastolic portion of the pressure–volume loops using a custom MATLAB program.[7] Three points were used for the exponential fit: (1) origin (0,0), (2) beginning diastolic point, and (3) end-diastolic point (Figure 1).[9] E_{ed} was obtained from the relation $\frac{dP}{dV}=\alpha\beta\cdot e^{\beta\times EDV}$ at calculated end-diastolic volumes. E_{ed} values were averaged for each animal.

Biaxial Biomechanical Evaluation

Square specimens were taken from the RV free wall myocardium and mounted on a biaxial testing device (CellScale Biomaterials Testing BioTester 5000) in modified Kreb's solution with 2,3-butanedione 2-monoxime and oxygen.[11,16] The Green-Lagrange strain tensor (R) and the second Piola-Kirchhoff stress tensor (S) were computed for each test protocol using standard methods,[16,17] with longitudinal and circumferential components given respectively by R_{LL}, S_{LL}, and R_{CC}, S_{CC}. Shear stresses S_{CL} were measured, but magnitudes were very small and were not used. Elastic modulus $\left(\frac{stress}{strain}\right)$ was extrapolated in both low- and high-strain regions (E_1 and E_2, respectively) for both the longitudinal and circumferential biaxial data by fitting a 2-branch function to the stress–strain data[14] (Figure 2):

$$Stress=\begin{cases} A*(e^{BE}-1), & E\le E_{ub} \\ A*(e^{BE_{ub}}-1)+AB*e^{BE_{ub}}(E-E_{ub}), & E\ge E_{ub} \end{cases},$$

$$\text{where } A=\frac{E_1}{B} \text{ and } B=\frac{\log\left(\frac{E_2}{E_1}\right)}{E_{ub}}$$

The first branch is exponential accounting for the accumulative stiffening of the tissue caused by gradual recruitment of collagen fibers, whereas the second branch is linear and reflects the behavior of the tissue after full strengthening of all collagen fibers. The parameter E_{ub} denotes the upper bound strain at which the transition between the 2 branches takes place and marks the beginning of a linear behavior with the modulus E_2. A counterpart to E_{ub} is the variable E_{lb}, which does not explicitly appear in our stress model. E_{lb} identifies the lower bound-strain region within which no significant portion of collagen fibers were yet recruited, and the behavior of the tissue was nearly linear, characterized by stiffness E_1. E_{lb} was estimated by detecting where the exponential branch deviated from a linear behavior.

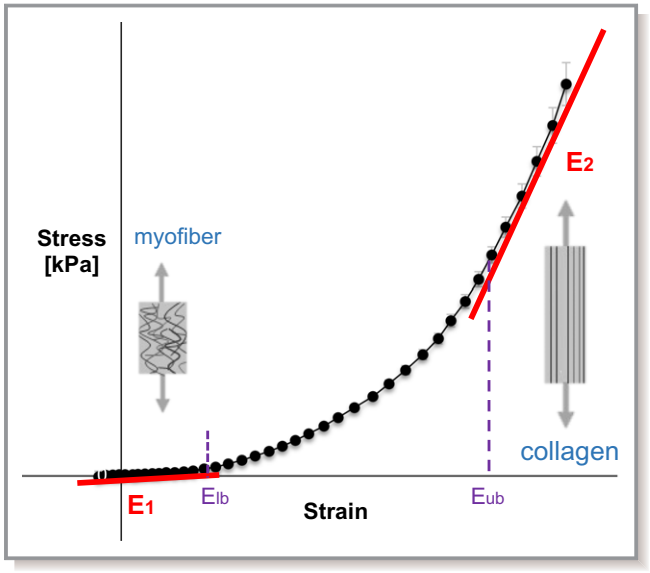

Figure 2. The E_1 region represents the elastic modulus in the low-strain, linear portion of the stress–strain curve at which collagen fibers have not yet been recruited and the behavior of the tissue is predominantly determined by myofibers. The E_2 region represents the elastic modulus in the high-strain, linear portion of the curve after all collagen fibers have straightened. E_{lb} indicates the lower boundary of the exponential transition region; E_{ub}, upper boundary of the exponential transition region.

Modeling the RV Wall Stress

The right ventricle in the PAB model was previously shown to have a decrease in ratio of longitudinal to circumferential length, suggesting change toward a spherical shape.[11] Consequently, the right ventricle was modeled as a sphere and wall stress was derived from pressure–volume data using the Laplace law[21]:

$$\text{Wall stress} = \frac{\text{Pressure} \times \text{radius}}{2 \times \text{thickness}}$$

The radius values were calculated from the conductance catheter-measured RV volume by the following relation for the volume of a sphere:

$$V = \frac{4}{3}\pi \times r^3$$

Wall thickness measurements were obtained from RV free wall square specimens and were assumed to be constant throughout the cardiac cycle. The calculated wall stress was plotted against the measured pressure values over the cardiac cycle.

Statistical Analyses

Results are reported as median and interquartile range (IQR; 25–75%). Control and PAB groups were compared using the Mann–Whitney test. $P<0.05$ was considered significant. The relationship between E_{ed} and stress–strain response was analyzed by plotting E_{ed} against the elastic modulus.

Results

A total of 7 control and 5 PAB rats were studied.

In Vivo Diastolic Hemodynamic Analysis

Pressure overload on the right ventricle significantly altered the pressure–volume relationship in the PAB rats compared with control (Figure 3A). PAB increased RV systolic pressure from 34.1 mm Hg (IQR: 31.1–36.6 mm Hg) in controls to 86.6 mm Hg (IQR: 74.7–101.5 mm Hg) in PAB models (P=0.003; Table). End-diastolic pressure was found to be significantly greater in PAB than control (10.3 mm Hg [IQR: 7.2–13.4 mm Hg] versus 5.5 mm Hg [IQR: 4.7–6.5 mm Hg]; P=0.005). E_{ed} was found to be significantly greater in PAB than control (146.6 mm Hg/mL [IQR: 105.8–155.0 mm Hg/mL] versus 55.1 mm Hg/mL [IQR: 44.7–85.4 mm Hg/mL]; P=0.010; Figure 3B). β was not found to be significantly different between PAB animals and control animals but had a positive correlation to E_{ed} (R=0.5954, P=0.04; Figure 4).

Biaxial Biomechanical Analysis

Biaxial mechanical analyses confirmed findings from prior studies (Table).[11] RV free wall thickness was significantly increased in PAB compared with control (1.29 mm [IQR: 1.26–1.46 mm] versus 0.66 mm [IQR: 0.63–0.71 mm]; P=0.003). The longitudinal stress–strain curve of the pressure-overloaded PAB model significantly shifted to the left, reflecting the increase in tissue stiffness in that direction (Figure 5A). Circumferential stress–strain curves showed no differences (Figure 5B), thus tissue anisotropy increased with PAB. Longitudinal E_1 was significantly increased in PAB compared with control (34.2 kPa [IQR: 18.1–44.6 kPa] versus 7.2 kPa [IQR: 6.7–18.1 kPa]; P=0.018; Figure 5C), whereas there was no significant change in E_2 (Figure 5D). There were no significant differences in E_1 or E_2 in the circumferential direction.

To illustrate the relationship between hemodynamic and biomechanical changes in diastolic stiffness, E_{ed} was plotted against longitudinal E_1 (Figure 6). An increase in E_{ed} was associated with an increase in longitudinal E_1 (R=0.3756).

Estimating Diastolic Wall Stress From Hemodynamic Data and Relating It to Biomechanical Data

Wall stress was calculated from the hemodynamic data via the Laplace law and then related to tissue stress derived from

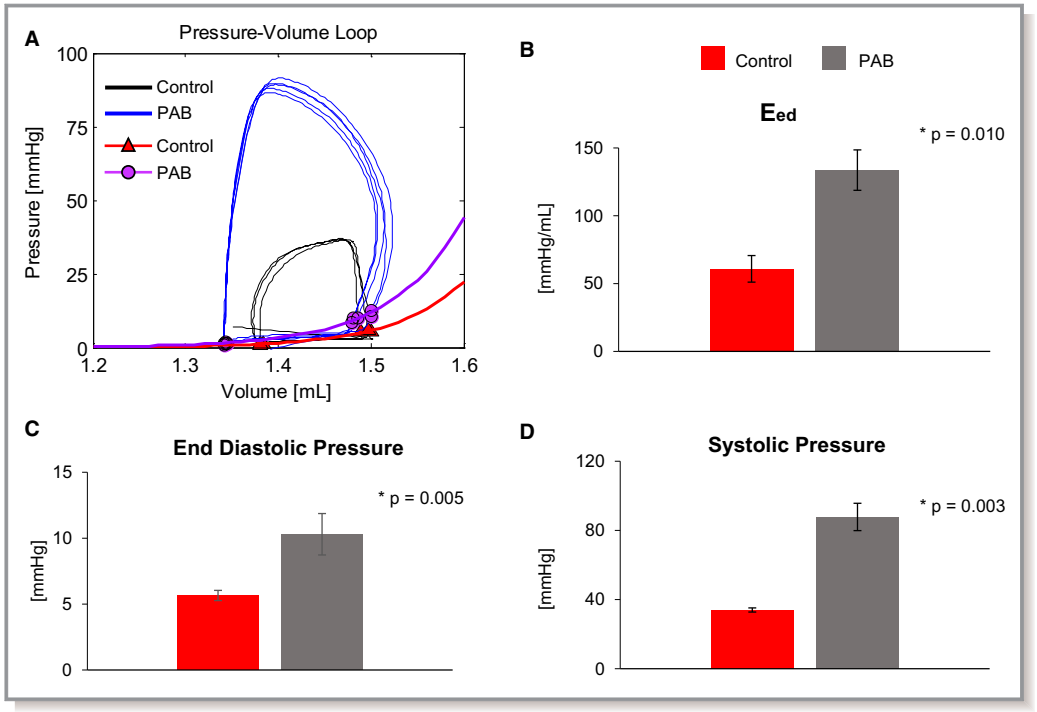

Figure 3. A, Representative pressure–volume loops for control and PAB demonstrate the significantly different diastolic pressure–volume relationship after 3 weeks of PAB. Triangular and circular points were representative diastolic points to fit the exponential curve to $P=\alpha\,(e^{\beta V}-1)$. B, Pressure overload on the right ventricle significantly increased end-diastolic elastance. C, PAB significantly increased end-diastolic pressure and (D) RV systolic pressure. Bar graphs represent mean values with error bars representing standard error. β indicates diastolic stiffness; E_{ed}, end diastolic elastance; P, pressure; PAB, pulmonary artery banding; RV, right ventricular; V, volume.

biomechanical testing. Plotting hemodynamically derived wall stress against RV pressure yielded stress–pressure loops in which the cardiac cycle can be viewed clockwise (Figures 7 and 8). Diastolic filling occurs at higher wall stress than isovolumetric relaxation. The calculated stress values were correlated to the ex vivo biomechanical stress–strain curves for each animal (Figure 7B). In both control and PAB animals, wall stress ranges estimated using the diastolic phase of the pressure–volume loop fell within both the E_1 zone and the transition zone (between E_1 and E_2), indicating that physiologically diastolic wall stiffness is composed of both a myofiber-predominant portion (early diastolic filling) and a combined myofiber and collagen portion (late diastolic filling). The biomechanical range of E_2 (collagen-only stiffness) was not reached in any part of physiological diastole.

Discussion

The objective of this study was to determine whether RV tissue biomechanical changes in the pressure-overloaded model would correlate with hemodynamic changes. More broadly, we wanted to answer the question of whether less invasive hemodynamic data could be used to predict biomechanical changes. We found that RV pressure overload in PAB rats resulted in an increase in diastolic myocardial stiffness reflected both hemodynamically, by an increase in E_{ed}, and biomechanically, by an increase in longitudinal E_1. These data, along with biomechanical analyses from prior studies, suggest that the PAB model preferentially induces RV myocardial tissue stiffening in the longitudinal direction[11] and that hemodynamic measurements could be used to predict biomechanical changes in the right ventricle. These results have translatable implications in studying disease pathology and monitoring treatment processes in patients with PH, as hemodynamic measurements are frequently obtained in patients, whereas myocardial tissue biopsies for biomechanical analysis are risky and not feasible.

Hemodynamically, the pressure overload in the PAB rat models was reflected in the significantly increased RV systolic pressure and resulted in significantly increased end-diastolic pressure and stiffness, measured by significantly increased E_{ed}. E_{ed} is a parameter that has been clinically linked to disease severity and linearly correlated to β in PAH patients.[8] The corresponding increases of E_{ed} in both patients and the PAB model suggest that this animal model has translational relevance in studying hemodynamic effects of RV remodeling

Table. Hemodynamic and Biomechanical Parameters

Parameter, Units	Control	PAB	*P* Value
Hemodynamic			
End-diastolic pressure, mm Hg	5.5 (4.7–6.5)	10.3 (7.2–13.4)	0.005*
Maximal systolic pressure, mm Hg	34.1 (31.1–36.6)	86.6 (74.7–101.5)	0.003*
End-diastolic elastance, mm Hg/mL	55.1 (44.7–85.4)	146.6 (105.8–155.0)	0.010*
β, mL^{-1}	10.5 (8.6–13.6)	13.2 (10.9–16.7)	0.429
Biomechanical			
RV free wall thickness, mm	0.66 (0.63–0.71)	1.29 (1.26–1.46)	0.003*
Longitudinal E_1, kPa	7.2 (6.7–18.1)	34.2 (18.1–44.6)	0.018*
Longitudinal E_2, kPa	653.7 (463.8–1054)	855.1 (702.3–1157.4)	0.343
Circumferential E_1, kPa	11.8 (7.1–16.5)	6.3 (5.4–8.6)	0.106
Circumferential E_2, kPa	713.9 (420.6–964.9)	514.1 (497.1–808)	1

Data reported as median (interquartile range; 25–75%). β indicates diastolic stiffness; E_1, elastic modulus in low-strain region; E_2, elastic modulus in high-strain region; PAB, pulmonary artery banding; RV, right ventricular.
*Denotes statistical significance of $P<0.05$.

in chronic pressure overload.[7,8] Interestingly, although we found β and E_{ed} to have a significant linear correlation, similar to prior reports, we did not find β to be significantly different between control and PAB animals. This disparity is likely due to a much wider range of calculated β, particularly in control animals. This may be caused by the method of volume normalization preferentially affecting the β analysis. Both β and E_{ed}, theoretically, are dependent volume measurements, given the expressions $P=\alpha\ (e^{\beta V}-1)$ and $E_{ed}=dP/dV=\alpha\beta\cdot e^{\beta\times EDV}$. However, E_{ed} is the slope of the change in pressure per change in volume (shown as dP/dV) and thus relies less on the relative volume and more on the shape of the pressure–volume loop. The shape of the pressure–volume loop itself is not altered in our volume-normalization protocol. For these reasons, E_{ed} may be a more practical parameter to report in animal studies.

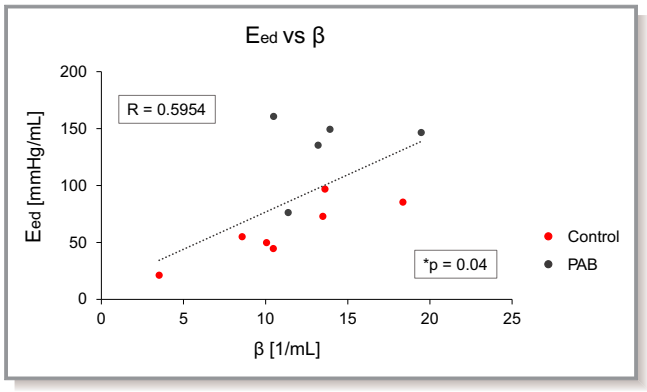

Figure 4. Plot of E_{ed} vs β showing a positive linear correlation with $R=0.5954$, $P=0.04$. E_{ed} indicates end-diastolic elastance; PAB, pulmonary artery banding; β, diastolic stiffness.

Biomechanically, the right ventricle had evidence of hypertrophy, as measured by significantly increased RV free wall thickness, and increased tissue stiffness in the longitudinal direction, as suggested by significantly greater longitudinal E_1. These results confirm our prior PAB studies that showed anisotropy (differential tissue stiffness in different directions of deformation) of the right ventricle under pressure overload.[11] The E_1 region of the stress–strain curve has been previously shown to represent myofiber stiffness (because the collagen fibers are not fully stretched and load bearing)[11,14] and suggests that tissue stiffness in the passive myocardium has contributions from the myofiber realignment and orientation. The lack of significant difference in the E_2 region of the stress–strain curve is also consistent with prior findings that this PAB rat model does not have significant histological changes in fibrosis.[11,12] These data also agree with single-cell tension studies of RV cardiomyocytes from PAH patients that showed increased passive tension and stiffness of the myofibers.[9] These corresponding results further suggest relevance of the PAB model for translational studies of the RV remodeling process in PAH and point to myofiber remodeling and biomechanics as a target of interest.

The stress–pressure loops provide a basis for dynamically studying biomechanical properties of the right ventricle. Relating RV wall stress modeling from in vivo hemodynamic data to ex vivo biomechanical testing of the RV myocardium suggests that diastolic filling occurs in 2 distinct biomechanical stress–strain ranges. Early diastolic filling (low pressure/stress) occurs at the myofiber predominant stress–strain region (E_1), and late diastolic filling (higher pressure/stress) occurs in the biomechanical transition zone involving both myofiber and collagen stiffness. The biomechanical stress–

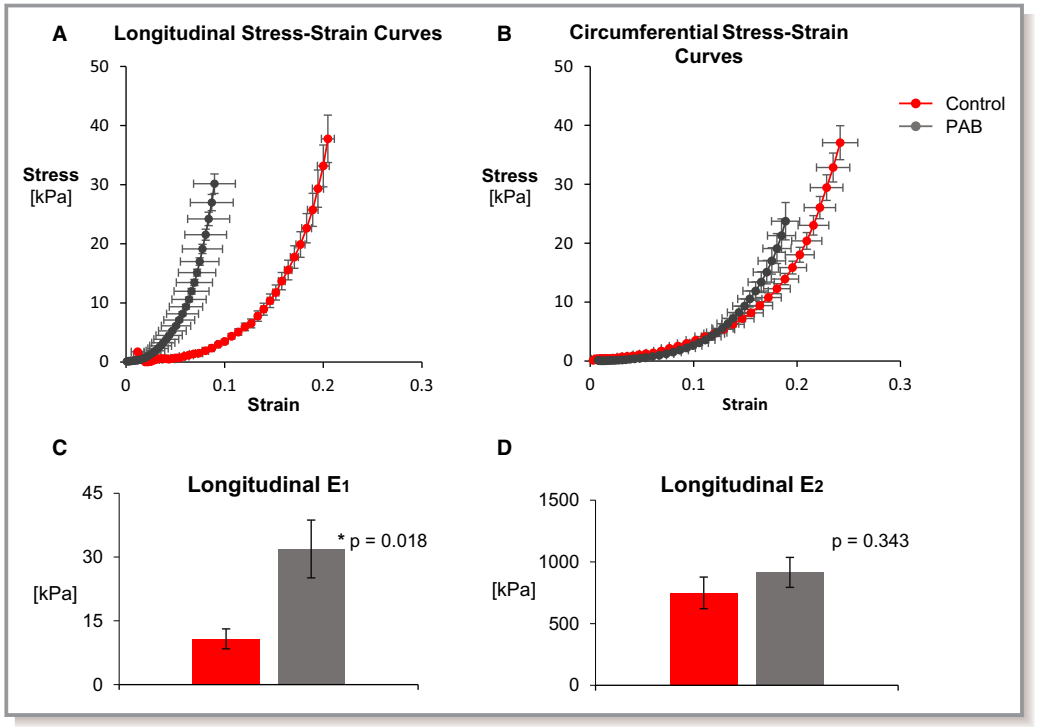

Figure 5. A, Average stress–strain curves in the PAB rats are shifted up and to the left in the longitudinal direction. Error bars represent standard error. B, There are no differences in the stress–strain curves in the circumferential direction. C, Longitudinal low-strain elastic modulus (E_1) was significantly increased in PAB rats. D, There was no significant difference in longitudinal high-strain elastic modulus (E_2). Bar graphs represent mean values with error bars representing standard error. PAB indicates pulmonary artery banding.

strain range dominated by complete collagen stretching is not seen physiologically in diastole. The calculated diastolic wall stresses fell consistently below the E_{ub}—or before the E_2 region—in both control and PAB. Because the E_2 region is thought to represent primarily collagen in the extracellular matrix, this suggests that collagen fibers in the RV myocardium do not fully stretch during diastole. This further implies that myofiber stiffness may be an important therapeutic target for PH.

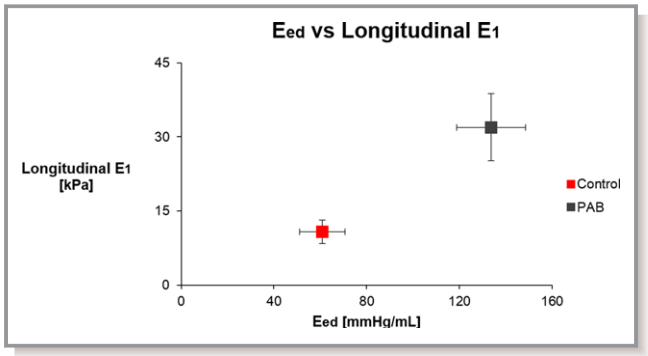

Figure 6. Integrating the hemodynamic changes in diastolic function with biomechanical changes in diastolic stiffness shows that PAB rats have both increased E_1 and E_{ed} with R=0.3856. Box represents mean E_{ed} and longitudinal E_1. Error bars represent standard error. E_1 indicates low-strain elastic modulus; E_{ed}, end-diastolic elastance; PAB, pulmonary artery banding.

Current available treatments for RV failure are targeted at reducing RV wall stress by lowering RV afterload. This can be accomplished by targeting extracardiac components using pulmonary arterial vasodilators such as endothelin receptor antagonists, prostanoids, and phosphodiesterase type 5 inhibitors. Targeting myocardial tissue stiffness and RV diastolic function may provide a unique treatment goal with few studies to date, mostly studying existing therapies not developed specifically for this purpose. In the PAB rat model, losartan and eplerenone lowered arterial pressures but did not have a significant effect on RV function or remodeling.[22] In contrast, sildenafil was found to have beneficial effects on systolic function and improved end-diastolic pressure without any effect on fibrosis.[23,24] Other studies have linked clinical presentation of the PAB model to other molecular targets of RV remodeling, such as overexpression of titin, heme oxigenase 1, and N2Ba; decreased fatty acid oxidation; capillary rarefication; and altered troponin phosphorylation and calcium handling.[25] The biomechanical–hemodynamic relationship may be a unique method to assess and guide therapeutic development of such novel myocardial targets.

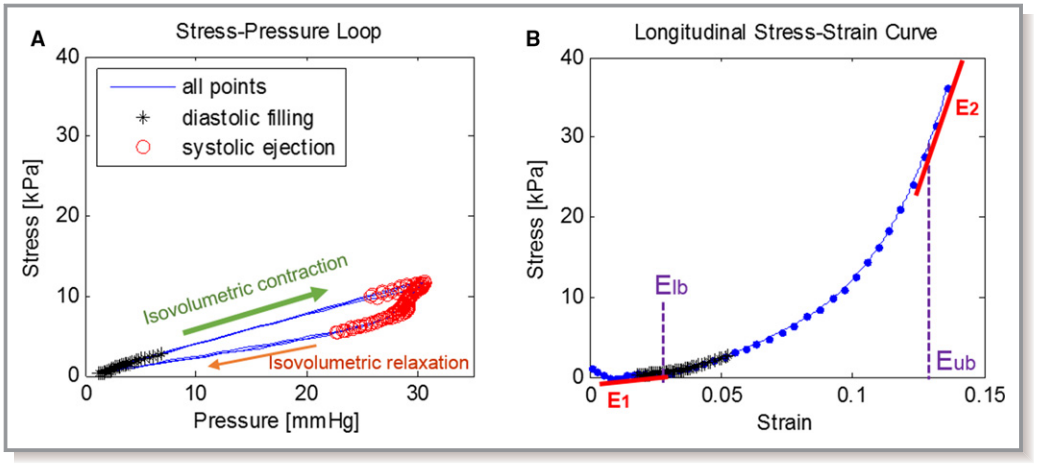

Figure 7. A, Plot of the measured pressure values against the calculated estimated wall stress using the Laplace model of a representative control animal. The black asterisks represent diastolic filling points, and the red circles represent the systolic ejection points. The rest of the cardiac cycle is labeled and progresses in a clockwise direction. B, Corresponding stress–strain curve of a representative control animal with black asterisks representing diastolic filling points. The purple dashed line indicates the E_{lb} and E_{ub} boundaries. E_1 and E_2 are represented by red lines in low- and high-strain regions, respectively. In this control animal, diastolic filling points overlap in both the E_1 and the exponential transitional area, suggesting predominant myofiber stretch involved in early diastolic filling followed by combined myofiber and collagen strengthening in late diastolic filling. E_1 indicates low-strain elastic modulus; E_2, high-strain elastic modulus; E_{lb}, lower boundary of the exponential transition region; E_{ub}, upper boundary of the exponential transition region.

A possible next step for translation for the biomechanical–hemodynamic link is to explore translation to noninvasive assessment by echocardiography. Echocardiography in combination with right heart catheterization has been used in prior clinical studies to calculate RV end-diastolic wall stress via the Laplace law.[26] In this method, the thickness of the RV free wall at end diastole can be obtained dynamically in patients via the subcostal view to provide real-time dimensional information for modeling throughout the cardiac cycle. Peak pressure can be estimated from Doppler velocity and the Bernoulli equation, which in turn can be used to estimate wall stress via the Laplace law with the RV spherical shape assumption.[27] Echocardiographic strain imaging by speckle tracking has also been compared with biomechanical strain for concomitant use in determining biomechanical properties and fiber orientation.[28] Limitations of echocardiography

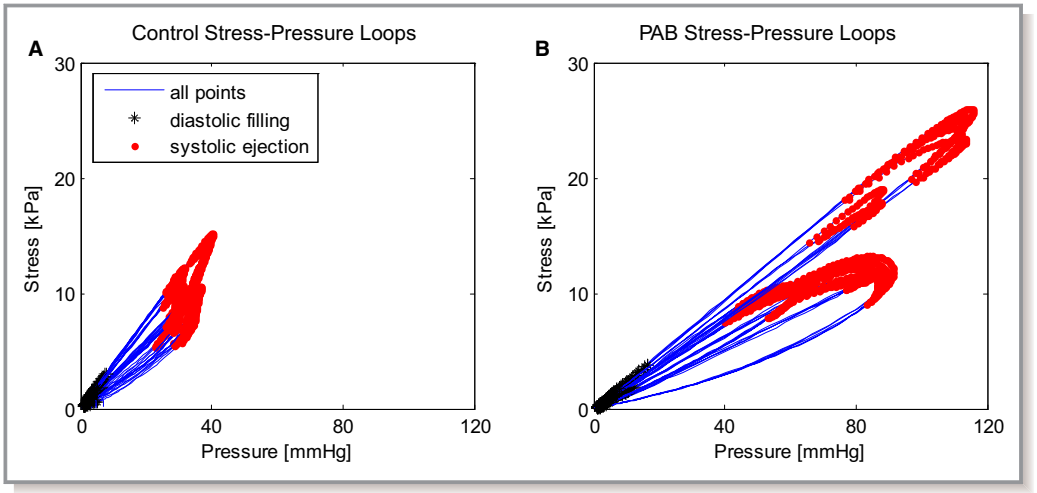

Figure 8. A, Plot of stress–pressure loops of all control animals. B, Plot of stress–pressure loops of all PAB animals. Black asterisks represent data points during diastolic filling, whereas red dots represent data points during systolic ejection. The cardiac cycle progresses in a clockwise direction. PAB indicates pulmonary artery banding.

potentially include the degree of error for velocity measurements with misalignment, incomplete RV imaging given its complex shape and proximity to the chest wall, and difficulty obtaining pressure values through the entire cardiac cycle.

Another topic of interest is the link between systolic and diastolic function. Both E_{ed} and end-systolic elastance have been shown to be elevated in patients with PAH, as well as in the PAB rat model.[8,11,25] RV diastolic dysfunction may be present in PAH despite compensated systolic function and is strongly linked to clinical outcomes.[7,8] The stress–pressure loops we present offer the ability to study biomechanical properties dynamically in both diastole and systole by pinpointing corresponding hemodynamic data and calculated stress to a specific portion of cardiac cycle. This information could be used to further elicit impact of myofiber or collagenous change on systolic, diastolic, or transitional function, as well as the relative contributions of the myofibers and extracellular matrix throughout the cardiac cycle. Recently, strain-area loops constructed from clinical echocardiographic data have been used to evaluate biomechanical properties dynamically throughout the cardiac cycle.[29,30] Similarly, our stress–pressure loops derived from hemodynamic data can be used to dynamically study the biomechanics under various physiologic states, for example, with exercise or vasodilatation. This is another path of translating our findings to the bedside to elicit more information about the relationship between the clinically relevant hemodynamic parameters and biomechanical properties of the myocardium at various disease stages.

This study has several limitations. We chose a PAB model specifically to evaluate changes in the right ventricle caused by pressure overload. This model is predominately one of myocyte hypertrophy and not fibrosis.[11,13] However, we show that diastolic filling occurs during the myocyte-dominated portion of the myocardial biomechanical function, making the PAB model particularly relevant to studying diastole. Other models of PAH, such as monocrotaline and Sugen-Hypoxia may provide additional insights but also have limitations regarding their applicability to clinical PAH. The monocrotaline model causes PH via metabolites of monocrotaline that injure the pulmonary vasculature and is predominantly a model of pulmonary arterial medial hypertrophy that is known to reverse quite easily with interventions.[31,32] The Sugen-Hypoxia model results in plexiform lesions in pulmonary arteries; however, development of RV failure is not consistent.[33,34]

Our hemodynamic analyses included normalization of end-diastolic volume to 1.5 mL of both control and PAB rats. This method is adapted from previous PAB rat model hemodynamic analyses[9] but has limitations of masking possible changes in volume to compensate for cardiac output and may have preferentially affected the calculation of β. Another limitation was that biomechanical studies were performed in 2 dimensions, not 3, which may limit interpretation; however, 3-dimensional biomechanical testing is not readily available currently. We previously studied stress–strain relationships across varying relative stress in the longitudinal and circumferential directions (ranging from ratios of 1:5 to 1:1 to 5:1), which allowed for calculation of tissue stiffness throughout the full 2-dimensional range and found the longitudinal direction to be stiffest.[16] The biomechanical studies are also limited in that they were conducted on passive and not actively contracting myocardium. Finally, wall stress modeling was performed with the assumption that the RV is spherical, which is consistent with histomorphologic studies of the PAB model that show changes from a high ellipsoidal to a more spherical morphology,[11] but does not account for regional differences. Further modeling may be possible to obtain estimated wall stress values that are more consistent with those of our animal model.

Conclusions

We examined the previously studied PAB rat model, which responds to pressure overload with myofiber hypertrophy. We found that a longitudinal elastic modulus calculated from biomechanical stress–strain studies of the RV free wall increased significantly, suggesting stiffer myofibers in the longitudinal direction. Functionally, this change was reflected in increased diastolic stiffness, as measured by hemodynamically derived elastance at the end diastole. Last, we modeled the right ventricle as a sphere and created a novel stress–pressure curve. The calculated diastolic wall stress range fell within the myofiber stretch and transitional portion of each animal's stress–strain curves, suggesting that collagen fibers were not fully stretched during diastole. Linking biomechanical findings with less invasive hemodynamics allowed us to study RV diastolic dysfunction at the tissue level. Similarly, the wall-stress loops modeled from hemodynamic data provided a way to dynamically study the right ventricle without requiring a myocardial tissue sample or biopsy.

Acknowledgments

The authors gratefully acknowledge surgical support from Jeff Baust, and technical support from Andrea Sebastiani and Sunaina Rustagi.

Sources of Funding

This work was supported by the American Heart Association (10BGIA3790022), the Pittsburgh Foundation (M2010-0052), and National Institutes of Health (P01 HL103455).

Disclosures

M.A.S.: Consultancy fees from United Therapeutics, Gilead, St. Jude Medical, Hoviione Sciencia, Actelion, Bayer. Research support from Novartis. S.J., R.R.V., R.A., E.L., T.N.B., M.S.: None.

References

1. D'Alonzo GE, Barst RJ, Ayres SM, Bergofsky EH, Brundage BH, Detre KM, Fishman AP, Goldring RM, Groves BM, Kernis JT, Levy PS, Pietra GG, Reid LM, Reeves JT, Rich S, Vreim CE, Williams GW, Wu M. Survival in patients with primary pulmonary hypertension. Results from a national prospective registry. *Ann Intern Med*. 1991;115:343–349.
2. Benza RL, Miller DP, Gomberg-Maitland M, Frantz RP, Foreman AJ, Coffey CS, Frost A, Barst RJ, Badesch DB, Elliott CG, Liou TG, McGoon MD. Predicting survival in pulmonary arterial hypertension: insights from the registry to evaluate early and long-term pulmonary arterial hypertension disease management (REVEAL). *Circulation*. 2010;122:164–172.
3. Ghio S, Klersy C, Magrini G, D'Armini AM, Scelsi L, Raineri C, Pasotti M, Serio A, Campana C, Vigano M. Prognostic relevance of the echocardiographic assessment of right ventricular function in patients with idiopathic pulmonary arterial hypertension. *Int J Cardiol*. 2010;140:272–278.
4. Chin KM, Kim NH, Rubin LJ. The right ventricle in pulmonary hypertension. *Coron Artery Dis*. 2005;16:13–18.
5. Vonk Noordegraaf A, Galie N. The role of the right ventricle in pulmonary arterial hypertension. *Eur Respir Rev*. 2011;20:243–253.
6. Thenappan T, Gomberg-Maitland M. Epidemiology of pulmonary hypertension and right ventricular failure in left heart failure. *Curr Heart Fail Rep*. 2014;11:428–435.
7. Vanderpool RR, Pinsky MR, Naeije R, Deible C, Kosaraju V, Bunner C, Mathier MA, Lacomis J, Champion HC, Simon MA. RV-pulmonary arterial coupling predicts outcome in patients referred for pulmonary hypertension. *Heart*. 2015;101:37–43.
8. Trip P, Rain S, Handoko ML, van der Bruggen C, Bogaard HJ, Marcus JT, Boonstra A, Westerhof N, Vonk-Noordegraaf A, de Man FS. Clinical relevance of right ventricular diastolic stiffness in pulmonary hypertension. *Eur Respir J*. 2015;45:1603–1612.
9. Rain S, Handoko ML, Trip P, Gan CT, Westerhof N, Stienen GJ, Paulus WJ, Ottenheijm CA, Marcus JT, Dorfmuller P, Guignabert C, Humbert M, Macdonald P, Dos Remedios C, Postmus PE, Saripalli C, Hidalgo CG, Granzier HL, Vonk-Noordegraaf A, van der Velden J, de Man FS. Right ventricular diastolic impairment in patients with pulmonary arterial hypertension. *Circulation*. 2013;128:2016–2025, 2011–2010.
10. Tuder RM, Marecki JC, Richter A, Fijalkowska I, Flores S. Pathology of pulmonary hypertension. *Clin Chest Med*. 2007;28:23–42, vii.
11. Hill MR, Simon MA, Valdez-Jasso D, Zhang W, Champion HC, Sacks MS. Structural and mechanical adaptations of right ventricle free wall myocardium to pressure overload. *Ann Biomed Eng*. 2014;42:2451–2465.
12. Bogaard HJ, Abe K, Vonk Noordegraaf A, Voelkel NF. The right ventricle under pressure: cellular and molecular mechanisms of right-heart failure in pulmonary hypertension. *Chest*. 2009;135:794–804.
13. Bogaard HJ, Natarajan R, Henderson SC, Long CS, Kraskauskas D, Smithson L, Ockaili R, McCord JM, Voelkel NF. Chronic pulmonary artery pressure elevation is insufficient to explain right heart failure. *Circulation*. 2009;120:1951–1960.
14. Avazmohammadi R, Hill MR, Simon MA, Zhang W, Sacks MS. A novel constitutive model for passive right ventricular myocardium: evidence for myofiber-collagen fiber mechanical coupling. *Biomech Model Mechanobiol*. 2017;16:561–581.
15. Horowitz A, Lanir Y, Yin FC, Perl M, Sheinman I, Strumpf RK. Structural three-dimensional constitutive law for the passive myocardium. *J Biomech Eng*. 1988;110:200–207.
16. Valdez-Jasso D, Simon MA, Champion HC, Sacks MS. A murine experimental model for the mechanical behaviour of viable right-ventricular myocardium. *J Physiol*. 2012;590:4571–4584.
17. Champion HC, Michelakis ED, Hassoun PM. Comprehensive invasive and noninvasive approach to the right ventricle-pulmonary circulation unit: state of the art and clinical and research implications. *Circulation*. 2009;120:992–1007.
18. Faber MJ, Dalinghaus M, Lankhuizen IM, Steendijk P, Hop WC, Schoemaker RG, Duncker DJ, Lamers JM, Helbing WA. Right and left ventricular function after chronic pulmonary artery banding in rats assessed with biventricular pressure-volume loops. *Am J Physiol Heart Circ Physiol*. 2006;291:H1580–H1586.
19. Suga H, Sagawa K. Instantaneous pressure-volume relationships and their ratio in the excised, supported canine left ventricle. *Circ Res*. 1974;35:117–126.
20. Lin DH, Yin FC. A multiaxial constitutive law for mammalian left ventricular myocardium in steady-state barium contracture or tetanus. *J Biomech Eng*. 1998;120:504–517.
21. Mauritz GJ, Vonk-Noordegraaf A, Kind T, Surie S, Kloek JJ, Bresser P, Saouti N, Bosboom J, Westerhof N, Marcus JT. Pulmonary endarterectomy normalizes interventricular dyssynchrony and right ventricular systolic wall stress. *J Cardiovasc Magn Reson*. 2012;14:5.
22. Borgdorff MA, Bartelds B, Dickinson MG, Steendijk P, Berger RM. A cornerstone of heart failure treatment is not effective in experimental right ventricular failure. *Int J Cardiol*. 2013;169:183–189.
23. Borgdorff MA, Bartelds B, Dickinson MG, van Wiechen MP, Steendijk P, de Vroomen M, Berger RM. Sildenafil treatment in established right ventricular dysfunction improves diastolic function and attenuates interstitial fibrosis independent from afterload. *Am J Physiol Heart Circ Physiol*. 2014;307:H361–H369.
24. Borgdorff MA, Bartelds B, Dickinson MG, Boersma B, Weij M, Zandvoort A, Sillje HH, Steendijk P, de Vroomen M, Berger RM. Sildenafil enhances systolic adaptation, but does not prevent diastolic dysfunction, in the pressure-loaded right ventricle. *Eur J Heart Fail*. 2012;14:1067–1074.
25. Borgdorff MA, Koop AM, Bloks VW, Dickinson MG, Steendijk P, Sillje HH, van Wiechen MP, Berger RM, Bartelds B. Clinical symptoms of right ventricular failure in experimental chronic pressure load are associated with progressive diastolic dysfunction. *J Mol Cell Cardiol*. 2015;79:244–253.
26. Addetia K, Sebag IA, Marelli A, Do DH, Afilalo J, Martucci G, Therrien J. Right ventricular end-diastolic wall stress: does it impact on right atrial size, and does it differ in right ventricular pressure vs volume loading conditions? *Can J Cardiol*. 2013;29:858–865.
27. Joyce JJ, Chang RK, Qi N, Owens TR, Ginzton LE, Baylen BG. Echocardiographic assessment of the right ventricular stress-velocity relationship under normal and chronic overload conditions. *Echocardiography*. 2004;21:17–25.
28. Yap CH, Park DW, Dutta D, Simon M, Kim K. Methods for using 3-D ultrasound speckle tracking in biaxial mechanical testing of biological tissue samples. *Ultrasound Med Biol*. 2015;41:1029–1042.
29. Lord R, George K, Somauroo J, Stembridge M, Jain N, Hoffman MD, Shave R, Haddad F, Ashley E, Jones H, Oxborough D. Alterations in cardiac mechanics following ultra-endurance exercise: insights from left and right ventricular area-deformation loops. *J Am Soc Echocardiogr*. 2016;29:879–887.e871.
30. Oxborough D, Heemels A, Somauroo J, McClean G, Mistry P, Lord R, Utomi V, Jones N, Thijssen D, Sharma S, Osborne R, Sculthorpe N, George K. Left and right ventricular longitudinal strain-volume/area relationships in elite athletes. *Int J Cardiovasc Imaging*. 2016;32:1199–1211.
31. Ruiter G, de Man FS, Schalij I, Sairras S, Grunberg K, Westerhof N, van der Laarse WJ, Vonk-Noordegraaf A. Reversibility of the monocrotaline pulmonary hypertension rat model. *Eur Respir J*. 2013;42:553–556.
32. Gomez-Arroyo JG, Farkas L, Alhussaini AA, Farkas D, Kraskauskas D, Voelkel NF, Bogaard HJ. The monocrotaline model of pulmonary hypertension in perspective. *Am J Physiol Lung Cell Mol Physiol*. 2012;302:L363–L369.
33. Ciuclan L, Bonneau O, Hussey M, Duggan N, Holmes AM, Good R, Stringer R, Jones P, Morrell NW, Jarai G, Walker C, Westwick J, Thomas M. A novel murine model of severe pulmonary arterial hypertension. *Am J Respir Crit Care Med*. 2011;184:1171–1182.
34. Toba M, Alzoubi A, O'Neill KD, Gairhe S, Matsumoto Y, Oshima K, Abe K, Oka M, McMurtry IF. Temporal hemodynamic and histological progression in Sugen5416/hypoxia/normoxia-exposed pulmonary arterial hypertensive rats. *Am J Physiol Heart Circ Physiol*. 2014;306:H243–H250.